A Structural Diversity of Molecular Alkaline-Earth-Metal Polyphosphides: From Supramolecular Wheel to Zintl Ion

Ravi Yadav[+,][a] Martin Weber[+,][b] Akhil K. Singh,[a] Luca Münzfeld,[a] Johannes Gramüller,[c] Ruth M. Gschwind,[c] Manfred Scheer,[b] and Peter W. Roesky*[a]

Abstract: A series of molecular group 2 polyphosphides has been synthesized by using air-stable $[Cp*Fe(\eta^5-P_5)]$ $(Cp* = C_5Me_5)$ or white phosphorus as polyphosphorus precursors. Different types of group 2 reagents such as organo-magnesium, mono-valent magnesium, and molecular calcium hydride complexes have been investigated to activate these polyphosphorus sources. The organo-magnesium complex $[(^{Dipp}BDI-Mg(CH_3))_2]$ $(^{Dipp}BDI = \{[2,6^{-i}Pr_2C_6H_3NCMe]_2CH\}^-)$ reacts with $[Cp*Fe(\eta^5-P_5)]$ to give an unprecedented Mg/Fe-supramolecular wheel. Kinetically controlled activation of

$[Cp*Fe(\eta^5-P_5)]$ by different mono-valent magnesium complexes allowed the isolation of Mg-coordinated formally mono- and di-reduced products of $[Cp*Fe(\eta^5-P_5)]$. To obtain the first examples of molecular calcium-polyphosphides, a molecular calcium hydride complex was used to reduce the aromatic $cyclo$-P_5 ring of $[Cp*Fe(\eta^5-P_5)]$. The Ca-Fe-polyphosphide is also characterized by quantum chemical calculations and compared with the corresponding Mg complex. Moreover, a calcium coordinated Zintl ion $(P_7)^{3-}$ was obtained by molecular calcium hydride mediated P_4 reduction.

Introduction

The recent years have witnessed a surge in the development of new methodologies for the transformation of white phosphorus (P_4) to valuable compounds.[1] The conventional methods for P_4 utilization involve toxic (Cl_2), corrosive (PCl_3), and pyrophoric (Na) reagents.[2] To circumvent such routes, the reductive functionalization of P_4 at ambient conditions by low-valent compounds offers an attractive alternative.[3] As a result, a variety of metal/non-metal coordinated P_n (n = 2 to 7) structural motifs have been obtained by a reductive approach. Despite a plethora of such polyphosphides, their further functionalization and utilization has been scarcely investigated.[4] The utilization of such stable polyphosphide-based systems instead of the

highly strained P_4 cage as a polyphosphorus source is an elegant approach (Figure 1a).

In a breakthrough report in 1987, Scherer and Brück successfully synthesized the air-stable pentaphosphaferrocene, $[Cp*Fe(\eta^5-P_5)]$, via co-thermolysis of $[(Cp*Fe(CO)_2)_2]$ and P_4.[5] The $cyclo$-P_5 ring in $[Cp*Fe(\eta^5-P_5)]$ has five lone pairs in C_5 symmetry and the Scheer group has advantageously utilized this property to pioneer a new area of inorganic supramolecular and coordination polymer chemistry.[6] Interestingly, the frontier molecular orbitals of $[Cp*Fe(\eta^5-P_5)]$ show significant contribution of the phosphorus atoms indicating the involvement of the $cyclo$-P_5 ring in redox events,[7] which has been confirmed by cyclic voltammetry[7b,8] and synthetically[7,9] as well. The air-stability and redox non-innocent nature of the $cyclo$-P_5 ring towards low-valent species makes $[Cp*Fe(\eta^5-P_5)]$ a suitable candidate as a polyphosphorus source. Very recently, we have used $[Cp*Fe(\eta^5-P_5)]$ to obtain E-phosphorus (E = Si, Ge, Al species) heterocyclic rings.[10]

Also, $[Cp*Fe(\eta^5-P_5)]$ shows nucleophilic-addition type reactivity towards various main group nucleophiles.[11] The reported examples of s-block polyphosphides, synthesised in solution or by solid-state routes, are dominated by group 1 elements.[12] Only a few structurally characterised group 2 polyphosphides are known.[13] This scarcity could be attributed to the instability of group 2 polyphosphides due to hard-soft mismatch and Schlenk equilibria. In 2016, Hill and co-workers reported molecular magnesium polyphosphides by the reaction of P_4 with organo-magnesium reagents.[14] To date this is the only report of group 2 element molecular polyphosphides.

In 2007, Jones and Stasch et al. reported a series of stable molecular mono-valent magnesium complexes.[15] Apart from being a fundamental breakthrough, Mg(I) complexes featuring a Mg–Mg bond have shown a wide range of potential applications due to their strong reducing nature. The selectivity

[a] Dr. R. Yadav,[+] Dr. A. K. Singh, L. Münzfeld, Prof. Dr. P. W. Roesky
Institute of Inorganic Chemistry
Karlsruhe Institute of Technology (KIT)
Engesserstraße 15, 76131 Karlsruhe (Germany)
E-mail: roesky@kit.edu

[b] M. Weber,[+] Prof. Dr. M. Scheer
Institute of Inorganic Chemistry
University of Regensburg
Universitätsstrasse 31, 93040 Regensburg (Germany).

[c] J. Gramüller, Prof. Dr. R. M. Gschwind
Institute of Organic Chemistry
University of Regensburg
Universitätsstrasse 31, 93040 Regensburg (Germany)

[+] These authors contributed equally to this manuscript.

💻 Supporting information for this article is available on the WWW under https://doi.org/10.1002/chem.202102355

Chemistry–A European Journal

Full Paper
doi.org/10.1002/chem.202102355

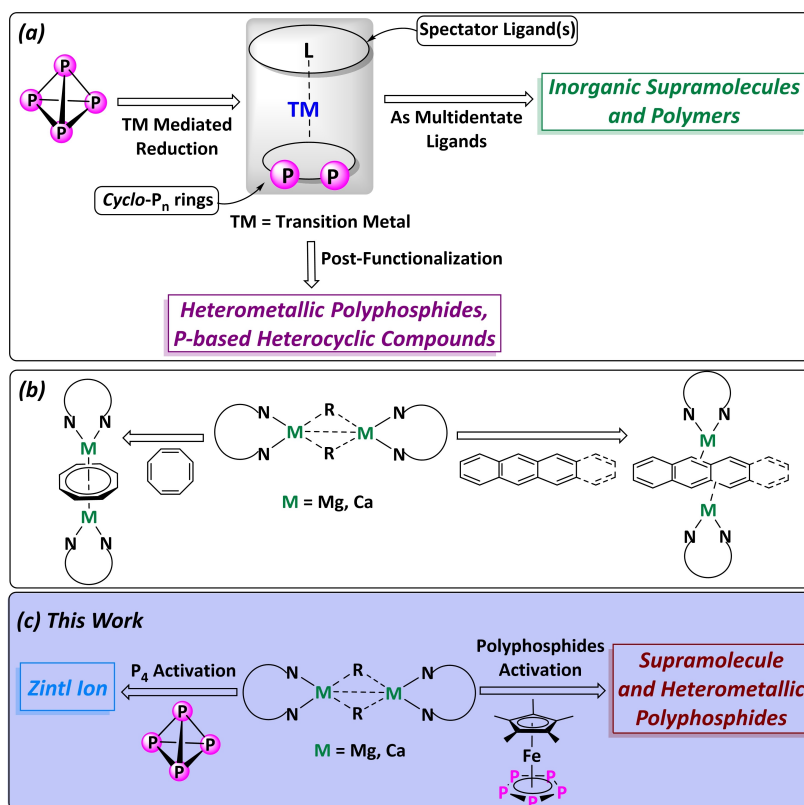**Chemistry Europe**
European Chemical
Societies Publishing

Figure 1. (a) TM mediated P_4 functionalization and its further use as ligands and as phosphorus source, (b) group 2 complexes as reductant for organic substrates, (c) overview of this work.

of Mg(I) compounds in reduction reactions has rendered them a promising class of reductants, and they have been promoted as "quasi-universal" reducing agents.[16] Recently, Schulz and co-workers used β-diketiminate coordinated Mg(I) with Pn_2R_4 (Pn = Sb, R = Me, Et; Pn = Bi, R = Ph) to isolate Mg-coordinated realgar type $[Pn_8]^{4-}$ polypnictides.[17] However, the reactivity of Mg compounds towards metal-coordinated polyphosphides has not been studied till date. Unlike Mg, monovalent-Ca species with a Ca–Ca bond is not yet known.[18] In 2006, Harder and co-workers reported the hydrocarbon-soluble molecular calcium hydride complex, $[\{(^{Dipp}BDI–Ca–H(thf)_2\}_2]$ ($^{Dipp}BDI = \{[2,6-^iPr_2C_6H_3NCMe]_2CH\}^-$),[19] to reduce organic substrates.[20] Very recently, Hill and co-workers have isolated trifold-coordinated $[(^{Dipp}BDI–Ca–H)_2]$[21] and used it to reduce alkenes,[22] cyclooctadiene,[23] and polyaromatic compounds.[24] Recently, the chemistry of molecular calcium compounds has witnessed a renaissance and a variety of neutral and cationic molecular calcium hydride complexes have been reported and used in small molecule activation and catalysis.[25]
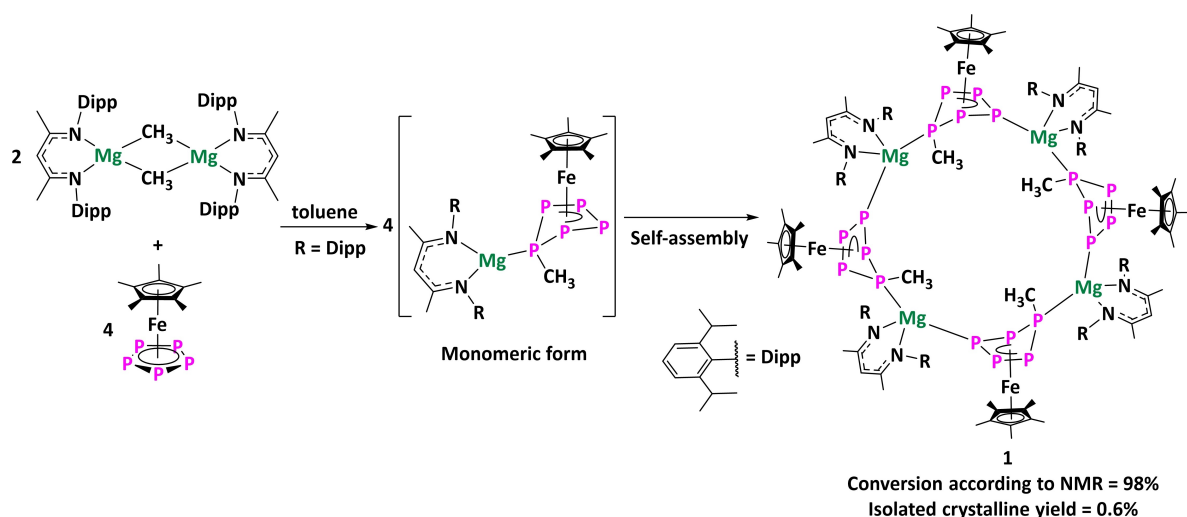
Herein, we report on the reactivity of $[Cp*Fe(\eta^5-P_5)]$ with β-diketiminate coordinated mono-valent magnesium compounds, resulting in the first examples of heterometallic Mg-polyphosphides. Also, the reactivity of β-diketiminate coordinated organo-magnesium compounds with $[Cp*Fe(\eta^5-P_5)]$ has been investigated to isolate an unprecedented Fe-supramolecular wheel assembled by Mg cations. Furthermore, the first ever example of a molecular calcium polyphosphide[26] has been

obtained by reducing $[Cp*Fe(\eta^5-P_5)]$ with molecular calcium hydride complex. The generality of the calcium hydride complex as a suitable reductant for polypnictogens has been established by accessing hydrocarbon soluble Ca-coordinated $[P_7]^{3-}$ Zintl ions by the controlled activation of P_4.

Results and Discussion

Magnesium polyphosphides

The addition of toluene to a mixture of one equivalent of $[(^{Dipp}BDI–Mg(CH_3))_2]$[27] and two equivalents of $[Cp*Fe(\eta^5-P_5)]$ at room temperature immediately resulted in a brown-coloured reaction mixture (Scheme 1). Monitoring the reaction by $^{31}P\{^1H\}$ NMR shows an AMM'XX' spin system and a singlet corresponding to some residual $[Cp*Fe(\eta^5-P_5)]$ (Figure S25). This spin system shows similarities to the NMR spectrum of the products isolated upon attack of alkali metal based nucleophiles on $[Cp*Fe(\eta^5-P_5)]$.[11] Therefore, it is likely that the reaction product in solution is $[Cp*Fe(\eta^4-P_5(CH_3))]^-$ with a $[^{Dipp}BDI–Mg]^+$ fragment attached to it. After removing the solvent and dissolving the brown residue in *n*-hexane and storing the resulting solution at −30 °C, crystals of a tetrameric Mg–Fe-polyphosphide species $[(^{Dipp}BDI–Mg)_4(\mu-\eta^{4:1:1}-P_5(CH_3))_4(FeCp*)_4]$ (**1**) were obtained (Figure 2). The tetrameric structure is built up from the self-assembly of the monomeric form by coordination of the

Chemistry–A European Journal

Full Paper
doi.org/10.1002/chem.202102355

Chemistry
Europe
European Chemical
Societies Publishing

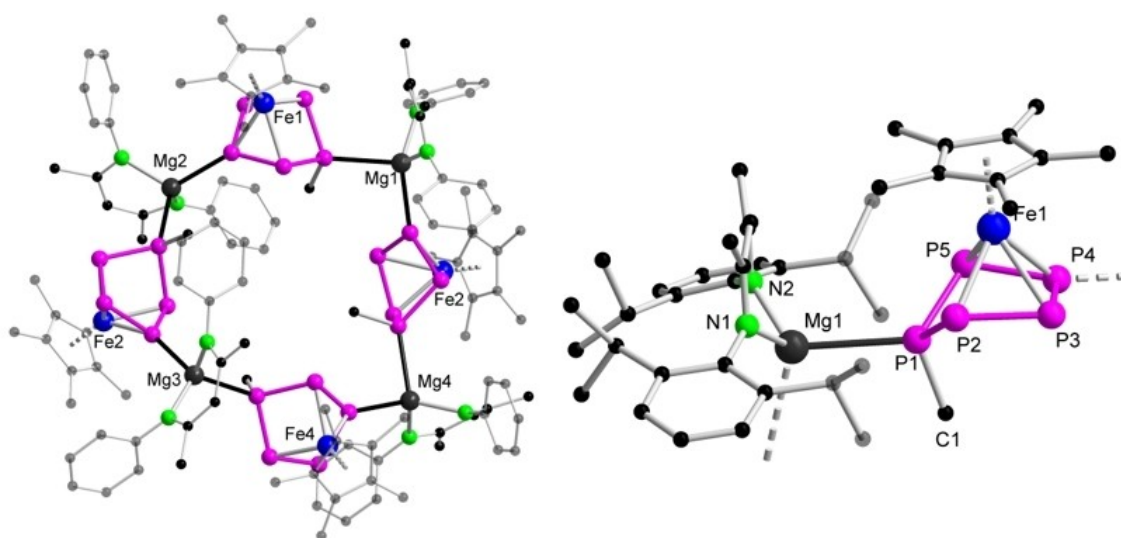**Scheme 1.** Synthesis of the Mg–Fe organo-polyphosphide supramolecular complex **1**.

Figure 2. Molecular structure of complex **1** (left) in the solid state (the isopropyl groups are omitted for clarity) and a view of the monomeric section of complex **1** (right). Hydrogen atoms are omitted for clarity. Selected bond lengths and angles are given in the Supporting Information.

[DippBDI–Mg]$^+$ fragment to the envelope-shaped *cyclo*-P$_5$ ring at 1,4 position. Complex **1** represents the largest supramolecular self-assembly of a s- and d-block heterometallic polyphosphide system. The tetrameric form could be arising from the combination of a coordinatively unsaturated Mg centre, the 1,4-coordination mode of the *cyclo*-P$_5$ ring and the sterically demanding DippBDI-ligand on the Mg atom. Also, complex **1** is the first example of a discrete cyclic tetrameric assembly based on pentaphosphaferrocene system.

The P–Mg–P angles deviate by 7° and twist angles between the planes of the unshifted phosphorus atoms of the *cyclo*-P$_5$-ligand (e.g. the plane [P3-P2-P5-P4] in Figure 2), deviates by more than 25°. Therefore, the tetramer itself is highly asymmetric. The monomeric units, as shown in Figure 2 have within the error range comparable bond lengths, but angles

within the *cyclo*-P$_5$ moieties differ slightly (up to more than 1°). The Mg–P bond distances in complex **1** are ranging from 2.5757(11) to 2.7676(11) Å and are in line with previous reports (2.5592(7)-2.831(3) Å).[14] The bond of the [DippBDI–Mg]$^+$ fragment to the unshifted 4-position of the *cyclo*-P$_5$-ring (average Mg–P 2.6004(11) Å) is shorter than the one with the methylated phosphorus atom (average Mg–P(CH$_3$) 2.7260(11) Å). This is in line with the assumption that the negative charge on the [(η^4-P$_5$(CH$_3$))] moiety is located primarily on the P$_4$ plane, as described for the known products of the reaction of main group nucleophiles on [Cp*Fe(η^5-P$_5$)].[11]

Since the ^{31}P{^{1}H} NMR spectrum of the reaction solution does not show a complex spin system but an AMM'XX' system with resonances $\delta = 142.6$ (m), 46.5 (m), −114.9 (m) ppm, we suggest that the tetramer **1** is not formed in solution. This was

Chemistry–A European Journal

Full Paper
doi.org/10.1002/chem.202102355

Chemistry
Europe
European Chemical
Societies Publishing

validated by Diffusion Ordered Spectroscopy (DOSY) NMR experiments, since the derived hydrodynamic volume of **1** (1748 ± 74 Å^3) is too small for a tetrameric or dimeric species and can rather be compared with the hydrodynamic volume of compound **2** (1339 ± 75 Å^3) (vide infa, for experimental details and diffusion coefficients see section 4, Supporting Information). Despite complete conversion of the reactants the crystalline yield of **1** is very low, which can be attributed to its high solubility in n-hexane and the dynamic process of self-assembly in solution.[28]

A different reaction was observed by treating [Cp*Fe(η^5-P$_5$)] with the mono-valent magnesium compound [(^{Dipp}BDI–Mg)$_2$].[15] Combining both precursors at room temperature led to an immediate colour change from green to dark brown (Scheme 2). Dark brown crystals of [(^{Dipp}BDI–Mg)$_2$(μ-η$^{4:2:1}$-P$_5$)(FeCp*))] (**2**) were isolated (Figure 3) by cooling a saturated pentane solution of the reaction mixture.

Complex **2** is formed by a two electron transfer from the Mg–Mg bond to one [Cp*Fe(η^5-P$_5$)] molecule, resulting in a formally twofold-reduced [Cp*Fe(η^4-P$_5$)]$^{2-}$ unit coordinated by two [^{Dipp}BDI–Mg]$^+$ moieties. When compared to other already reported [Cp*Fe(η^4-P$_5$)]$^{2-}$ motifs, such as [K(dme)K(dibenzo-[18]crown-6)][Cp*Fe(η^4-P$_5$)],[7b] the *cyclo*-P$_5$ ring in **2** is highly asymmetric due to the coordination of Mg2 to the P3 atom. Compared to the sum of the covalent radii for Mg–P single (2.50 Å) and double (2.34 Å) bonds,[29] the bond lengths Mg1–P1 (2.4627(6) Å) and Mg2-P1 (2.5452(6) Å) lie in the range
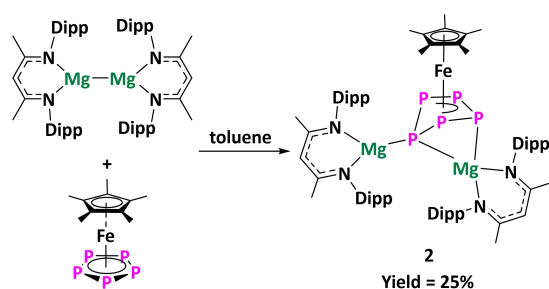
of a single bond and are similar to known Mg–P bonds for example [Mg(PSi^{t}Bu$_3$)]$_6$ (2.474(2) Å)[30] and [Mg{(P(H)Si^{i}Pr$_2$)$_2$O}(thf)]$_3$ (2.557(2) Å).[31] However, electrostatic interactions and packing effects play a significant role. The long Mg2–P3 (2.6764(6) Å) bond distance indicates a relatively weaker interaction also observed in [(PNNP)Mg]$_2$ (2.6737(12) Å; PNHNHP = N,N-bis(2-(diphenyl-phosphino)phenyl)ethane-1,2-diaine).[32]

The ^{31}P{^{1}H} NMR spectrum of complex **2** shows four broad signals and one well-resolved triplet at room temperature. Upon cooling the solution, the broad signals start splitting up (coalescence temperature at about 0 °C) until an ADMOX spin system is best resolved at −40 °C (Figure S26).

The ^{1}H NMR spectrum also shows a dynamic behaviour, since for the isopropyl groups of the (^{Dipp}BDI) ligands only an extremely broad signal is observed at room temperature, which splits up into a septet at −40 °C (Figure S4–7). In order to identify all coupling constants in the ^{31}P{^{1}H} NMR spectrum, the ADMOX spin system resonances at $\delta = 66.5$, 59.3, −8.4, −22.8, and −54.6 ppm at −40 °C were simulated (see Table S2 and Figure S26). Due to the line broadening at these temperatures, only one ^2J-coupling was resolved (linewidth for all signals larger than 25 Hz). The dynamic behaviour, which is seen in the ^{31}P{^{1}H} NMR spectrum is a result of electrostatic interaction between Mg and P. The multiplets in the low temperature ^{31}P{^{1}H} NMR can be assigned to the corresponding phosphorus atoms in the solid state structure (Table S2) by simulation of the ADMOX spin system.

Interestingly, VT NMR-experiments showed no difference when the reaction between [(^{Dipp}BDI–Mg)$_2$] and [Cp*Fe(η^5-P$_5$)] was started at either −80 °C or room temperature and there was no hint for the formation of a formally mono-reduced [P$_{10}$]$^{4-}$ moiety. Also, when the reaction between [(^{Dipp}BDI–Mg)$_2$] and [Cp*Fe(η^5-P$_5$)] in 1:2 molar ratio was carried out at either −80 °C or room temperature only complex **2** is observed. We assume that the radical intermediate, [(^{Dipp}BDI–Mg)(μ-η^4-P$_5$)(FeCp*))], is too bulky to dimerize via a P–P bond formation (see below). Instead, the intermediate is reduced a second time.

To support this hypothesis, we employed the less bulky Mg reagent [(^{Mes}BDI–Mg)$_2$][33] (^{Mes}BDI = {[2,4,6-Me$_3$C$_6$H$_3$NCMe]$_2$CH}$^-$) to reduce [Cp*Fe(η^5-P$_5$)]. In fact, the reaction between [(^{Mes}BDI–Mg)$_2$] with [Cp*Fe(η^5-P$_5$)] in a 1:2 molar ratio leads to the formation of [(^{Mes}BDI–Mg)$_2$(μ-η$^{4:4:2:2}$-P$_{10}$)(FeCp*)$_2$] (**3**) (Scheme 3). The molecular structure showed the formation of a

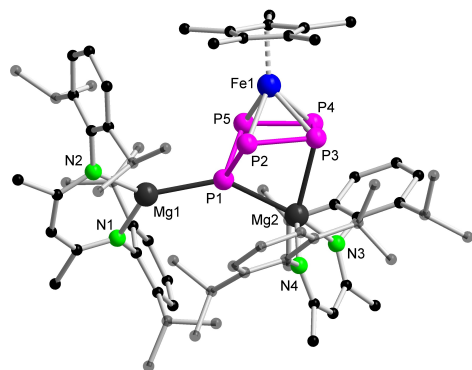**Scheme 2.** Synthesis of complex **2**.

Figure 3. Molecular structure of complex **2** in the solid state. Hydrogen atoms are removed for clarity. Selected bond lengths and angles are given in the Supporting Information.
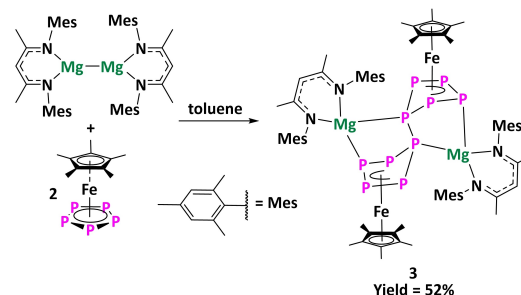
Scheme 3. Synthesis of complex **3**.

Chemistry–A European Journal

Full Paper
doi.org/10.1002/chem.202102355

Chemistry Europe
European Chemical
Societies Publishing

$[P_{10}]^{4-}$ fragment, η^4-coordinated to two $[Cp*Fe]^+$ and η^2-coordinated to two $[^{Mes}BDI-Mg]^+$ moieties (Figure 4). Similar $[(\eta^4-P_{10})(FeCp*)_2]^{2-}$ moieties have been obtained coordinated to potassium or samarium ions upon reduction of $[Cp*Fe(\eta^5-P_5)]$ by potassium hydride and divalent samarocene, respectively.[7b,9] A similar P_{10} moiety has also been reported in an organo-cobalt compound.[34] The Mg1-P7 (2.5879(14) Å), Mg1-P3 (2.639(2) Å), Mg2-P1 (2.577(2) Å), and Mg2-P9 (2.613(2) Å) bond lengths are similar to those observed in previously reported magnesium polyphosphide complexes (2.5592(7)–2.831(3) Å).[14] The Mg1···P2 (3.142(2) Å) and Mg2···P8 (3.192(2) Å) separations are however significantly longer than the Mg–P bonds reported in the literature (2.45-2.99 Å), precluding a bonding interaction between P10 and Mg1 on the one hand, and P3 and Mg2 on the other hand.[35] The P–P bond lengths (2.154(2)–2.172(2) Å) within the *cyclo*-P_5 ring are intermediate between single and double bonds, indicating a partial double-bond character.[36] The distance of the newly formed P5–P6 bond (2.1992(13) Å) in **3** is also slightly shorter than the analogous P–P bond in $[(Cp*_2Sm)_2(\mu-\eta^{4:4}-P_{10})(FeCp*)_2]$ (2.2089(13) Å).[9] The formation of complex **3** can be explained by the transfer of two electrons from the Mg–Mg dimer to two molecules of $[Cp*Fe(\eta^5-P_5)]$. As a result, two radical iron species with the unpaired electron localized on one P atom of the *cyclo*-P_5 ring are generated in situ and subsequently dimerize through the coupling of the radicals resulting in the formation of a P–P bond, which is now sterically not hindered like in the case of **2**. Moreover, this transformation is accompanied by a conformational change of the *cyclo*-P_5 rings, from planar to envelope-shaped. The ^1H NMR spectrum of complex **3** shows a downfield shift for the protons of the Cp* group, from δ 1.08 to 1.21 ppm, compared to $[Cp*Fe(\eta^5-P_5)]$ (Figure S11). The protons of the (^{Mes}BDI) ligands coordinated to the magnesium centres are also shifted downfield. For example, the o-CH_3 of the mesityl group are shifted from δ 1.91 ppm in $[(^{Mes}BDI-Mg)_2]$ to δ 2.53 ppm in complex **3**.[37] The $^{31}P\{^1H\}$ NMR spectrum confirms the formation of a $[P_{10}]^{4-}$ moiety by the presence of four resonances at δ −30.6
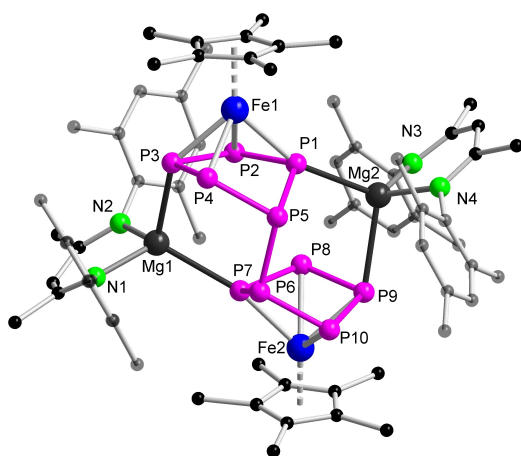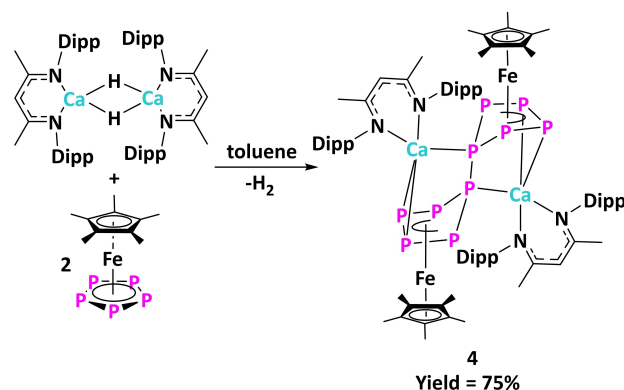
(br, $\Delta\nu_{1/2} \approx 600$ Hz), 24.5 (br, $\Delta\nu_{1/2} \approx 550$ Hz), 126.5 (br, $\Delta\nu_{1/2} \approx 500$ Hz), and 152.1 (br, $\Delta\nu_{1/2} \approx 500$ Hz) ppm. Unfortunately, the P–P coupling constants could not be determined as finely resolved $^{31}P\{^1H\}$ NMR spectra could not be obtained even at low temperature (-80 °C) due to the low solubility of **3** at low temperatures and the fluxional behaviour of the $[P_{10}]^{4-}$ fragment (Figure S12-13). Complex **3** slowly decomposes to unidentified products at room temperature, both in solution and in the solid-state. However, no decomposition was observed when stored at −40 °C for at least 4–5 weeks.

Calcium polyphosphides

After the investigation of $[Cp*Fe(\eta^5-P_5)]$ with organo-magnesium and monovalent-magnesium reducing agents, we were intrigued to study the next heavier alkaline earth metal calcium for comparison. Surprisingly, to the best of our knowledge, there is no structurally characterized example known of calcium polyphosphides.[26] The Mg-polyphosphide complexes (**1**-**3**) are stabilized by efficient kinetic- and thermodynamic-stabilization by bulky β-diketiminate ligands. We envisaged to use $[(^{Dipp}BDI-Ca-H)_2]$ to reduce $[Cp*Fe(\eta^5-P_5)]$, where the [Ca–H] unit reduces the aromatic polyphosphide ring and the bulky β-diketiminate ligand stabilizes the resulting Ca-polyphosphide species.

Upon addition of toluene to a mixture of $[(^{Dipp}BDI-Ca-H)_2]$ and $[Cp*Fe(\eta^5-P_5)]$ in a 1:2 molar ratio immediate change from green to dark brown along with the liberation of gas H_2 occurred (Scheme 4). After workup, dark coloured crystals of $[(^{Dipp}BDI-Ca)_2(\mu-\eta^{4:4:3:3}-P_{10})(FeCp*)_2]$ (**4**) were isolated in 75% yield. Complex **4** is formed by a formal mono-reduction of $[Cp*Fe(\eta^5-P_5)]$ accompanied by dihydrogen liberation. Notably, complex **4** is the first example of a structurally characterized calcium-coordinated polyphosphide. A similar reaction was observed when KH was reacted with $[Cp*Fe(\eta^5-P_5)]$ to give $[\{K(DME)_2\}\{K(DME)\}(\mu-\eta^4-P_{10})(FeCp*)_2]$ as a polymer, however.[7b]

Apart from a remarkable extension of polyphosphides to calcium, the better solubility of complex **4** compared to that of $[\{K(DME)_2\}\{K(DME)\}(\mu-\eta^4-P_{10})(FeCp*)_2]$ in hydrocarbon solvents with low-polarity, such as toluene or benzene, could be an

Figure 4. Molecular structure of complex **3** in the solid state. Hydrogen atoms and the non-coordinating solvent molecules are removed for clarity. Selected bond distances and angles are given in the Supporting Information.

Scheme 4. Synthesis of complex **4**.

Chemistry–A European Journal

Full Paper
doi.org/10.1002/chem.202102355

**Chemistry
Europe**
European Chemical
Societies Publishing

advantage for its further utility as polyphosphide transfer agent. In contrast to complex **3**, the two *cyclo*-P_5 units in complex **4** are completely in a *trans* arrangement (Figure 5).

In complex **4** each [(^{Dipp}BDI–Ca)]$^+$ moiety is η^3-coordinated to the [(μ-η^4-P_{10})(FeCp*)$_2$] fragment. The Ca–P1 (2.9605(8) Å)
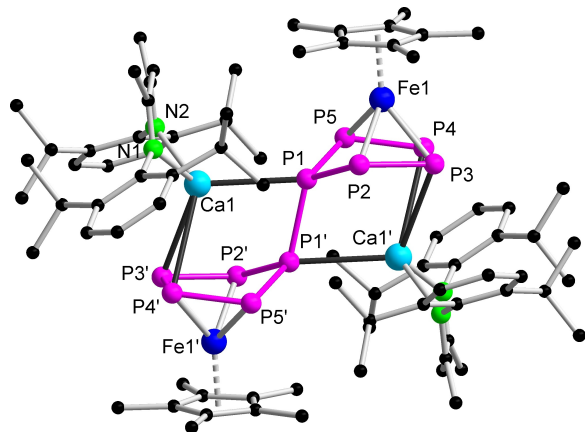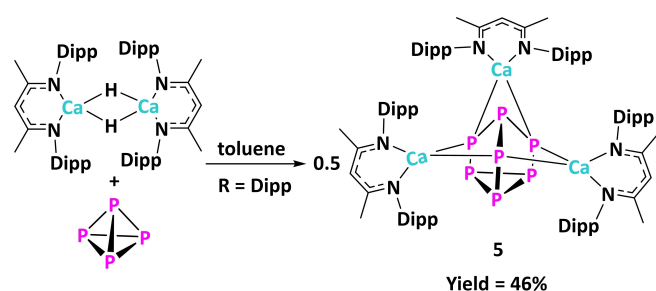

Figure 5. Molecular structure of complex **4** in the solid state. Hydrogen atoms and the non-coordinating solvent molecules are removed for clarity. Selected bond distances and angles are given in the Supporting Information.

Scheme 5. Synthesis of complex **5**.

and Ca–P3 (2.9748(8) Å) bond lengths are comparable to [(Me$_3$Si)$_2$NCa[P(H)(Si^{i}Pr$_3$)]$_3$Ca(thp)$_3$] (thp = tetrahydropyran) (2.882(2)–2.978(4) Å).[38] The Ca–P4 bond distance (3.1430(8) Å) indicates a weak interaction. The P–P bond distances (2.1488(11)–2.1767(10) Å) within *cyclo*-P_5 rings are similar to complex **3**. The P1–P1′ (2.3455(12) Å) bond connecting two halves is significantly longer than in complex **3** (2.1992(13) Å).

The ^{1}H NMR spectrum of complex **4** confirmed the C_2 symmetric nature as per the solid-state structure (Figure S15). Similarly to complex **3**, the ^{31}P{^{1}H} NMR spectrum of **4** at room temperature also showed broad resonances at δ = -21.0 (br), −18.7 (br), 152.4 (br), 182.3 (br) ppm due to the fluxional coordination of the [(^{Dipp}BDI–Ca)]$^+$ moiety within the (P_{10}) framework. Unfortunately, recording the ^{31}P{^{1}H} NMR at low temperature did not give any better resolution due to low solubility at low temperatures and strong dynamic behaviour (cf. Figure S16–17).

After the reduction of the transition metal polyphosphide, [Cp*Fe(η^5-P_5)], with a molecular calcium hydride, we were challenged to establish the generality of [(^{Dipp}BDI–Ca–H)$_2$] as a suitable reductant for the synthesis polypnictogen complexes. In this context, we employed [(^{Dipp}BDI–Ca–H)$_2$] for the reduction of P_4 (Scheme 5). The reaction of [(^{Dipp}BDI–Ca–H)$_2$] with P_4 resulted in two major products as evidenced by the ^{31}P{^{1}H} NMR spectrum of the crude reaction mixture (Figure S20). After work-up, [(^{Dipp}BDI–Ca)$_3$(μ-$\eta^{2:2:2}$-P_7)] (**5**) was isolated in pure form as pale-yellow coloured crystals in 46% yield. Unfortunately, the second product formed along with complex **5** with a resonance at −241.3 ppm in the ^{31}P{^{1}H} NMR spectrum could not be isolated, and its identity remains elusive. The molecular structure of complex **5** showed the formation of a (P_7)$^{3−}$ Zintl ion encapsulated by three [(^{Dipp}BDI–Ca)]$^+$ moieties (Figure 6). The Ca–P bond lengths in complex **5** are in the range of 2.8667(9)–2.9346(9) Å which are similar to those in previously reported examples, such as [^{Dipp}BDI–Ca-PPh$_2$(thf)] (2.872(4) Å),[39] [(Me$_3$Si)$_2$NCa[P(H)(Si^{i}Pr$_3$)]$_3$Ca(thp)$_3$] (2.882(2)–2.978(4) Å).[38] The
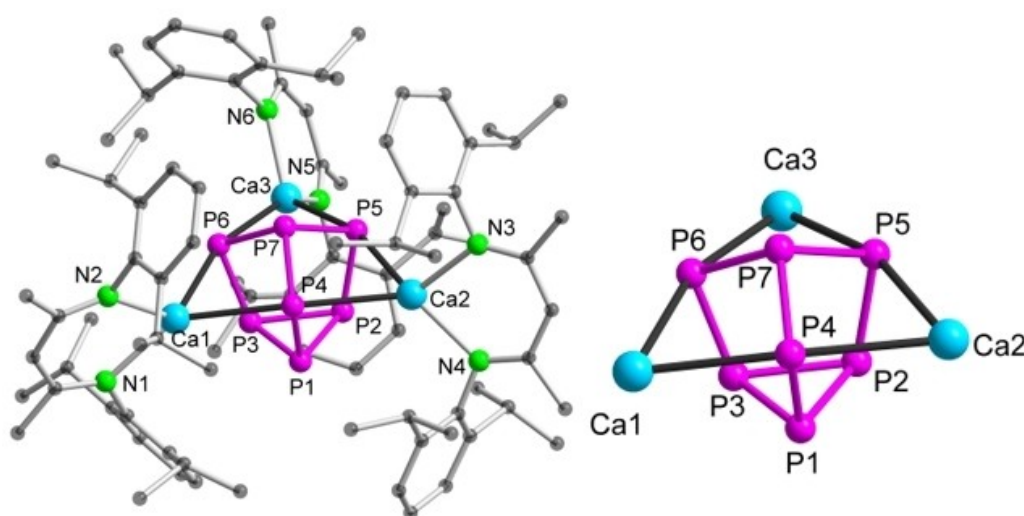

Figure 6. Molecular structure of complex **5** (left) in the solid state and a view of **5** (right) without β-diketiminate moieties of the core structure. Hydrogen atoms and the non-coordinating solvent molecules are removed for clarity. Selected bond distances and angles are given in the Supporting Information.

Chemistry–A European Journal

Full Paper
doi.org/10.1002/chem.202102355

Chemistry
Europe
European Chemical
Societies Publishing

P—P bond distances (2.1748(10)–2.2586(11) Å) in the (P$_7$)-cage are in the expected range for such a nortricyclane-like cage.[12] Complex **5** is the first structurally characterized molecular calcium-coordinated pnictogen Zintl ion. Molecular group 2 based Zintl ions are very challenging to obtain in a pure form and reasonable yield. Previously, Hill *et al.* reported the reaction between [(^{Mes}BDI—Mg-*n*-butyl] and P$_4$ to give [(^{Mes}BDI—Mg)$_3$(μ-η$^{2:2:2}$-P$_7$)] in 5% yield along with other unidentified products.[14]

The ^{1}H NMR spectrum of complex **5** showed a single set of resonances for the different chemical groups indicating a symmetric arrangement of the [(^{Dipp}BDI—Ca)]$^+$ moieties around the (P$_7$)$^{3-}$ ion in solution (Figure S19). The room temperature ^{31}P{^{1}H} NMR spectrum of complex **5** showed a very broad resonance at δ = −87.7 ppm. Upon measuring VT ^{31}P{^{1}H} NMR spectra, the broad resonance transformed to three new signals at δ = −137.8 (br, Δν$_{1/2}$ ≈ 430 Hz, 3P), −60.5 (br, Δν$_{1/2}$ ≈ 570 Hz, 3P), and −40.9 (br, m, 1P) ppm at −90 °C (Figure S22), which are in line with previous reports of {P$_7$}$^{3-}$ species showing three sets of resonances δ = -162 (3P), −103 (3P), and −57 (1P) ppm at −60 °C.[12] However, ^{n}J$_{PP}$ coupling constants were not observed as the strong dynamics could not be suppressed even at −90 °C, which is due to the rapid rearrangement (similar to bullvalene) within (P$_7$)$^{3-}$ in solution.[12] An NMR scale reaction between [(^{Dipp}BDI—Ca—H)$_2$] and P$_4$ showed a very broad resonance at δ = −87.7 ppm corresponding to complex **5** and an unidentified by-product at δ = −241.3 ppm (Figure S20). In contrast, the reaction of [(^{Dipp}BDI—Mg—H)$_2$] with P$_4$ led to the formation of a primary magnesium phosphide, [(^{Dipp}BDI—Mg-μ-PH$_2$)$_3$], PH$_3$, and several other unidentified species.[14] Mézailles *et al.* have reacted LiB(Et)$_3$H with P$_4$ to obtain [(TMEDA—Li)$_3$(P$_7$)] (TMEDA = tetramethylethylenediamine) along with [LiPH$_2${B-(Et)$_3$}].[40] Complex **5** is stable at room temperature in the solid state and in solution (benzene, toluene) under inert conditions for at least two weeks. However, storing for longer periods shows the formation of (^{Dipp}BDI—H) and an insoluble precipitate.

Molecular modeling

The geometries of the (P$_{10}$) moieties in the solid-state structures of complexes **3** (*eclipsed*) and **4** (*trans*) are different. There can be three possible factors; 1) crystal packing 2) ligand bulkiness i.e. mesityl vs. di-isopropyl groups on the BDI ligands, and 3) effect of different ion Mg vs. Ca. A series of density functional theory (DFT) calculations have been carried out by using the Gaussian 16 package[43] to get more insights at the UB97D[44]/LANL2DZ/6-31G** level. The geometries of complexes **3** and **4** were optimized (Figure 7). The calculated frontier molecular orbitals are given in the Supporting Information. The calculations revealed that the solid-state geometries are also retained in gas phase. Two different types of geometries of the (P$_{10}$) moiety are also found in optimized structures as we have observed in the corresponding crystal structures of **3** and **4**. Owing to this, the role of crystal packing to stabilize different geometries can be excluded. We have also calculated the ground state energy for the two different geometries of [(Cp*)$_2$Fe$_2$P$_{10}$]$^{2-}$ moiety after removing the corresponding [^{R}BDI—M] (R = Mes, M = Mg; R = Dipp, M = Ca) ions and the fully *trans* geometry was found to be 6 kcal/mol more stable than the eclipsed conformation. This is also reflected in the relatively more thermal stability of complex **4** (trans conformation) than that of **3** (eclipsed conformation). We have also optimized complex **3Ca** and **4Mg** by replacing the metal ions in complex **3** and **4** with Ca and Mg, respectively. The enthalpies and free energies have been compared for all four possible complexes (Table S4). The free energies of complexes **3Mg** and **3Ca** are nearly equal however, complex **4Ca** display 6 kcal/mol less free energy than complex **4Mg**. This further support the feasible formation of *trans* isomer by calcium ion. To examine the role of ligand bulkiness, (^{Mes}BDI (**3**) vs. ^{Dipp}BDI (**4**)), to stabilize such different geometries we have also optimized complex **4** without side chain isopropyl groups of the phenyl ring while keeping other things intact, at the same level of theory. The calculation showed no conformational change which further clarifies that
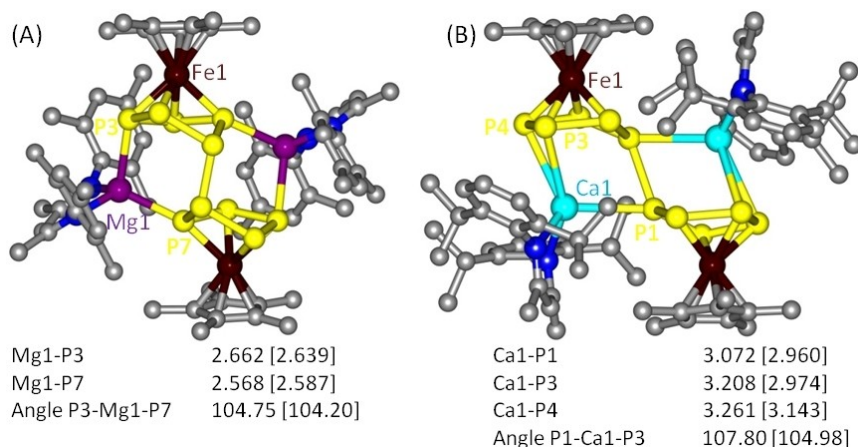

(A)		
Mg1-P3	2.662 [2.639]	
Mg1-P7	2.568 [2.587]	
Angle P3-Mg1-P7	104.75 [104.20]	

(B)		
Ca1-P1	3.072 [2.960]	
Ca1-P3	3.208 [2.974]	
Ca1-P4	3.261 [3.143]	
Angle P1-Ca1-P3	107.80 [104.98]	

Figure 7. UB97D optimized geometries of complex **3** (A) and complex **4** (B) with bond lengths in Å and angles in degree as calculated using LANL2DZ basis set for iron, magnesium and calcium atom and 6–31G** for all other atoms. Parentheses contain the experimental value obtained from the respective X-ray structures.

Chemistry–A European Journal

Full Paper
doi.org/10.1002/chem.202102355

Chemistry Europe
European Chemical
Societies Publishing

there is no role of the ligand bulkiness in stabilization of different geometries (Figure S32).

The topological analysis of the electron density within the framework of Bader's theory (QTAIM)[45] analysis of complex **3** and **4** were also performed. The value of electron density ρ and the sign of Laplacian distribution $\nabla^2\rho(r)$ at bond critical point (BCP) are closely related to bonding strength and nature of interaction respectively in any pair of interacting atoms.[46] The values of several relevant parameters for selected bond pairs are summarized in Table 1. The strength of such interactions were also determined according to the method proposed by Espinosa *et al.*[41] and Vener *et al.*[42] Based on the crystal structure data and the aforementioned guideline of QTAIM analysis, we found that in complex **3**, each Mg atom binds with only two P atoms, whereas each Ca atom binds with three P atoms in complex **4** (Figure 8). Hence, the different topologies of the (P_{10}) moieties in **3** and **4** can be attributed to the more coordination of Ca to P atoms as compared to Mg due to the larger ion size.

Conclusions

We have synthesized a series of molecular group 2 polyphosphides by using $[Cp^*Fe(\eta^5\text{-}P_5)]$ as an air-stable polyphosphorus source. The organo-magnesium reagent, $[(^{Dipp}BDI\text{–}Mg(CH_3))_2]$, reacts with $[Cp^*Fe(\eta^5\text{-}P_5)]$ in a nucleophilic-addition-type reaction resulting in $[\{(^{Dipp}BDI\text{–}Mg)(\mu\text{-}\eta^4\text{-}P_5(CH_3)(FeCp^*)\}]$ (in situ) which, upon crystallization, undergoes self-assembly to give an unprecedented Mg/Fe-polyphosphide supramolecular wheel (**1**). Complex **1** is the first example of a discrete cyclic-tetrameric assembly based on a pentaphosphaferrocene system. The different reactivity of mono-valent magnesium complexes demonstrates the role of ancillary ligand bound to the Mg centre on the outcome of the resulting polyphosphide. In case of $[(^{Dipp}BDI\text{–}Mg)_2]$, the formally twofold-reduced product **2** was obtained exclusively, whereas, upon employing $[(^{Mes}BDI\text{–}Mg)_2]$, featuring a slightly lower steric demand, the formally mono-reduced species P_{10}^{2-} species **3** could be isolated. The polyphosphide chemistry is remarkably extended to previously unknown calcium-polyphosphide. The sterically encumbered molecular calcium hydride $[(^{Dipp}BDI\text{–}Ca\text{–}H)_2]$ proved to be a suitable reductant for diverse polyphosphorus systems. The aromatic *cyclo*-P_5 ring in $[Cp^*Fe(\eta^5\text{-}P_5)]$ was readily reduced by $[(^{Dipp}BDI\text{–}Ca\text{–}H)_2]$ to selectively give the formally mono-reduced product **4**. The subtle changes in the polyphosphide topology upon changing the alkaline-earth-metal ion (Mg (**3**) vs. Ca (**4**)) were also analysed by theoretical calculations. The activation of P_4 by $[(^{Dipp}BDI\text{–}Ca\text{–}H)_2]$ resulted in complex **5** in which a phosphorus Zintl ion is coordinated by calcium atoms for the first time in a molecular species. The use of $[(^{Dipp}BDI\text{–}Ca\text{–}H)_2]$ as an efficient reductant for polyphosphide systems opens new avenues for heavy alkaline earth metal polypnictogenides.

Table 1. Topological parameters of electron density: electron density [$\rho(r)$], its Laplacian distribution [$\nabla^2\rho(r)$], potential energy density [$V(r)$], and kinetic energy density [$G(r)$] at the selected bond critical points (3, −1), All parameters are in atomic units (a.u.).

Atom pairs	Electron Density $\rho(r)$	Laplacian Distribution $\nabla^2\rho$	Potential Energy Density $V(r)$	Kinetic Energy Density $G(r)$	Interaction Energy [kcal/mol] E_{int}[a]	E_{int}[b]
Mg1-P3	0.026	0.111	−0.010	0.006	3.38	1.67
Mg1-P7	0.021	0.092	−0.008	0.005	2.80	1.53
Ca1-P1	0.017	0.063	−0.013	0.014	4.37	4.01
Ca1-P3	0.018	0.068	−0.015	0.016	4.80	4.36
Ca1-P4	0.004	0.017	−0.004	0.004	1.32	1.16

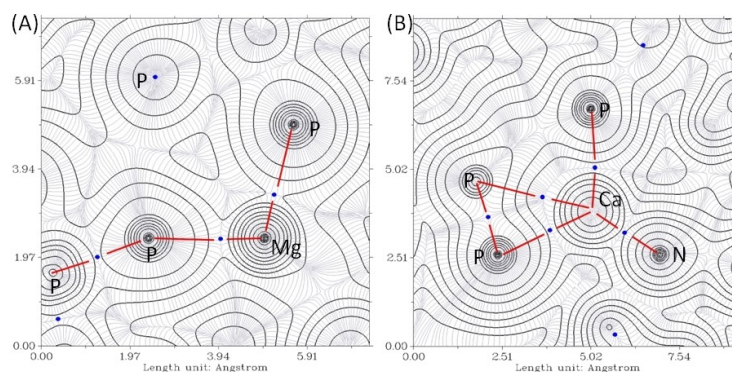E_{int}[a] $= -V(r)/2$.[41] E_{int}[b] $= 0.429 G(r)$.[42]

Figure 8. QTAIM analysis of (A) complex **3** and (B) complex **4**. Contour line plots of the electron density showing bond critical points between selected atom pairs.

Experimental Section

General experimental procedures for the synthesis of all compounds, characterization, quantum chemical calculations and X-ray crystallography are described in the Supporting Information.

Deposition Number(s) 2050401 (**1**), 2050402 (**2**), 2050403 (**3**), 2050404 (**4**), and 2050405 (**5**) contain(s) the supplementary crystallographic data for this paper. These data are provided free of charge by the joint Cambridge Crystallographic Data Centre and Fachinformationszentrum Karlsruhe Access Structures service.

Conflict of Interest

The authors declare no conflict of interest.

[1] a) D. H. R. Barton, J. Zhu, *J. Am. Chem. Soc.* **1993**, *115*, 2071–2072; b) D. H. R. Barton, R. A. Vonder Embse, *Tetrahedron* **1998**, *54*, 12475–12496; c) Y. H. Budnikova, D. G. Yakhvarov, O. G. Sinyashin, *J. Organomet. Chem.* **2005**, *690*, 2416–2425; d) B. M. Cossairt, C. C. Cummins, *New J. Chem.* **2010**, *34*, 1533–1536; e) J. E. Borger, A. W. Ehlers, J. C. Slootweg, K. Lammertsma, *Chem. Eur. J.* **2017**, *23*, 11738–11746; f) S. K. Ghosh, C. C. Cummins, J. A. Gladysz, *Org. Chem. Front.* **2018**, *5*, 3421–3429; g) U. Lennert, P. B. Arockiam, V. Streitferdt, D. J. Scott, C. Rödl, R. M. Gschwind, R. Wolf, *Nat. Catal.* **2019**, *2*, 1101–1106; h) G. Lu, J. Chen, X. Huangfu, X. Li, M. Fang, G. Tang, Y. Zhao, *Org. Chem. Front.* **2019**, *6*, 190–194.

[2] D. E. C. Corbridge, *Phosphorus 2000. Chemistry, biochemistry & technology*, Elsevier, Amsterdam, **2000**.

[3] a) M. Caporali, L. Gonsalvi, A. Rossin, M. Peruzzini, *Chem. Rev.* **2010**, *110*, 4178–4235; b) B. M. Cossairt, N. A. Piro, C. C. Cummins, *Chem. Rev.* **2010**, *110*, 4164–4177; c) M. Scheer, G. Balázs, A. Seitz, *Chem. Rev.* **2010**, *110*, 4236–4256; d) L. Xu, Y. Chi, S. Du, W.-X. Zhang, Z. Xi, *Angew. Chem. Int. Ed.* **2016**, *55*, 9187–9190; *Angew. Chem.* **2016**, *128*, 9333–9336; e) S. Du, J. Yin, Y. Chi, L. Xu, W.-X. Zhang, *Angew. Chem. Int. Ed.* **2017**, *56*, 15886–15890; *Angew. Chem.* **2017**, *129*, 16102–16106; f) S. Du, J. Yang, J. Hu, Z. Chai, G. Luo, Y. Luo, W.-X. Zhang, Z. Xi, *J. Am. Chem. Soc.* **2019**, *141*, 6843–6847; g) B. van Ijzendoorn, M. Mehta, *Dalton Trans.* **2020**, *49*, 14758–14765; h) D. Sarkar, C. Weetman, D. Munz, S. Inoue, *Angew. Chem. Int. Ed.* **2021**, *60*, 3519–3523; *Angew. Chem.* **2021**, *133*, 3561–3565.

[4] C. M. Hoidn, D. J. Scott, R. Wolf, *Chem. Eur. J.* **2021**, *27*, 1886–1902.

[5] O. J. Scherer, T. Brück, *Angew. Chem. Int. Ed.* **1987**, *26*, 59; *Angew. Chem.* **1987**, *99*, 59.

[6] a) J. Bai, A. V. Virovets, M. Scheer, *Science* **2003**, *300*, 781–783; b) M. Scheer, L. J. Gregoriades, A. V. Virovets, W. Kunz, R. Neueder, I. Krossing, *Angew. Chem. Int. Ed.* **2006**, *45*, 5689–5693; *Angew. Chem.* **2006**, *118*, 5818–5822; c) M. Scheer, A. Schindler, R. Merkle, B. P. Johnson, M. Linseis, R. Winter, C. E. Anson, A. V. Virovets, *J. Am. Chem. Soc.* **2007**, *129*,

13386–13387; d) M. Scheer, *Dalton Trans.* **2008**, 4372–4386; e) M. Scheer, A. Schindler, C. Gröger, A. V. Virovets, E. V. Peresypkina, *Angew. Chem. Int. Ed.* **2009**, *48*, 5046–5049; *Angew. Chem.* **2009**, *121*, 5148–5151; f) A. Schindler, C. Heindl, G. Balázs, C. Gröger, A. V. Virovets, E. V. Peresypkina, M. Scheer, *Chem. Eur. J.* **2012**, *18*, 829–835; g) C. Schwarzmaier, A. Schindler, C. Heindl, S. Scheuermayer, E. V. Peresypkina, A. V. Virovets, M. Neumeier, R. Gschwind, M. Scheer, *Angew. Chem. Int. Ed.* **2013**, *52*, 10896–10899; *Angew. Chem.* **2013**, *125*, 11097–11100.

[7] a) T. Li, J. Wiecko, N. A. Pushkarevsky, M. T. Gamer, R. Köppe, S. N. Konchenko, M. Scheer, P. W. Roesky, *Angew. Chem. Int. Ed.* **2011**, *50*, 9491–9495; *Angew. Chem.* **2011**, *123*, 9663–9667; b) M. V. Butovskiy, G. Balázs, M. Bodensteiner, E. V. Peresypkina, A. V. Virovets, J. Sutter, M. Scheer, *Angew. Chem. Int. Ed.* **2013**, *52*, 2972–2976; *Angew. Chem.* **2013**, *125*, 3045–3049.

[8] R. F. Winter, W. E. Geiger, *Organometallics* **1999**, *18*, 1827–1833.

[9] T. Li, M. T. Gamer, M. Scheer, S. N. Konchenko, P. W. Roesky, *Chem. Commun.* **2013**, *49*, 2183–2185.

[10] a) R. Yadav, B. Goswami, T. Simler, C. Schoo, S. Reichl, M. Scheer, P. W. Roesky, *Chem. Commun.* **2020**, *56*, 10207–10210; b) R. Yadav, T. Simler, B. Goswami, C. Schoo, R. Köppe, S. Dey, P. W. Roesky, *Angew. Chem. Int. Ed.* **2020**, *59*, 9443–9447; *Angew. Chem.* **2020**, *132*, 9530–9534; c) R. Yadav, T. Simler, S. Reichl, B. Goswami, C. Schoo, R. Köppe, M. Scheer, P. W. Roesky, *J. Am. Chem. Soc.* **2020**, *142*, 1190–1195.

[11] E. Mädl, M. V. Butovskii, G. Balázs, E. V. Peresypkina, A. V. Virovets, M. Seidl, M. Scheer, *Angew. Chem. Int. Ed.* **2014**, *53*, 7643–7646; *Angew. Chem.* **2014**, *126*, 7774–7777.

[12] R. S. P. Turbervill, J. M. Goicoechea, *Chem. Rev.* **2014**, *114*, 10807–10828.

[13] a) W. Dahlmann, H. G. v. Schnering, *Naturwissenschaften* **1972**, *59*, 420–420; b) N. Korber, J. Daniels, *Z. Anorg. Allg. Chem.* **1999**, *625*, 189–191.

[14] M. Arrowsmith, M. S. Hill, A. L. Johnson, G. Kociok-Köhn, M. F. Mahon, *Angew. Chem. Int. Ed.* **2015**, *54*, 7882–7885; *Angew. Chem.* **2015**, *127*, 7993–7996.

[15] S. P. Green, C. Jones, A. Stasch, *Science* **2007**, *318*, 1754–1757.

[16] a) A. Stasch, C. Jones, *Dalton Trans.* **2011**, *40*, 5659–5672; b) C. Jones, *Nat Rev Chem* **2017**, *1*, 0059.

[17] a) C. Ganesamoorthy, C. Wölper, A. S. Nizovtsev, S. Schulz, *Angew. Chem. Int. Ed.* **2016**, *55*, 4204–4209; *Angew. Chem.* **2016**, *128*, 4276–4281; b) J. Krüger, C. Wölper, S. Schulz, *Inorg. Chem.* **2020**, *59*, 11142–11151.

[18] S. Krieck, H. Görls, L. Yu, M. Reiher, M. Westerhausen, *J. Am. Chem. Soc.* **2009**, *131*, 2977–2985.

[19] S. Harder, J. Brettar, *Angew. Chem. Int. Ed.* **2006**, *45*, 3474–3478; *Angew. Chem.* **2006**, *118*, 3554–3558.

[20] a) J. Spielmann, S. Harder, *Chem. Eur. J.* **2007**, *13*, 8928–8938; b) J. Spielmann, F. Buch, S. Harder, *Angew. Chem. Int. Ed.* **2008**, *47*, 9434–9438; *Angew. Chem.* **2008**, *120*, 9576–9580; c) J. Spielmann, S. Harder, *Eur. J. Inorg. Chem.* **2008**, 1480–1486; d) J. Intemann, H. Bauer, J. Pahl, L. Maron, S. Harder, *Chem. Eur. J.* **2015**, *21*, 11452–11461.

[21] A. S. S. Wilson, M. S. Hill, M. F. Mahon, C. Dinoi, L. Maron, *Science* **2017**, *358*, 1168–1171.

[22] A. S. S. Wilson, M. S. Hill, M. F. Mahon, *Organometallics* **2019**, *38*, 351–360.

[23] M. S. Hill, M. F. Mahon, A. S. S. Wilson, C. Dinoi, L. Maron, E. Richards, *Chem. Commun.* **2019**, *55*, 5732–5735.

[24] A. S. S. Wilson, C. Dinoi, M. S. Hill, M. F. Mahon, L. Maron, E. Richards, *Angew. Chem. Int. Ed.* **2020**, *59*, 1232–1237; *Angew. Chem.* **2020**, *132*, 1248–1253.

[25] D. Mukherjee, D. Schuhknecht, J. Okuda, *Angew. Chem. Int. Ed.* **2018**, *57*, 9590–9602; *Angew. Chem.* **2018**, *130*, 9736–9749.

[26] W. Dahlmann, H. G. v. Schnering, *Naturwissenschaften* **1973**, *60*, 518–518.

[27] A. P. Dove, V. C. Gibson, P. Hormnirun, E. L. Marshall, J. A. Segal, A. J. P. White, D. J. Williams, *Dalton Trans.* **2003**, 3088–3097.

[28] A. Wiesner, S. Steinhauer, H. Beckers, C. Müller, S. Riedel, *Chem. Sci.* **2018**, *9*, 7169–7173.

[29] P. Pyykkö, S. Riedel, M. Patzschke, *Chem. Eur. J.* **2005**, *11*, 3511–3520.

[30] M. Westerhausen, M. Krofta, A. Pfitzner, *Inorg. Chem.* **1999**, *38*, 598–599.

[31] P. Kopecky, C. von Hänisch, F. Weigend, A. Kracke, *Eur. J. Inorg. Chem.* **2010**, 258–265.

[32] S. Bestgen, C. Schoo, B. L. Neumeier, T. J. Feuerstein, C. Zovko, R. Köppe, C. Feldmann, P. W. Roesky, *Angew. Chem. Int. Ed.* **2018**, *57*, 14265–14269; *Angew. Chem.* **2018**, *43*, 14461–14465.

[33] S. J. Bonyhady, C. Jones, S. Nembenna, A. Stasch, A. J. Edwards, G. J. McIntyre, *Chem. Eur. J.* **2010**, *16*, 938–955.

[34] O. J. Scherer, T. Völmecke, G. Wolmershäuser, *Eur. J. Inorg. Chem.* **1999**, 945–949.

[35] C. R. Groom, I. J. Bruno, M. P. Lightfoot, S. C. Ward, *Acta Crystallogr. Sect. B* **2016**, *72*, 171–179.

[36] P. Pyykkö, M. Atsumi, *Chem. Eur. J.* **2009**, *15*, 186–197.

[37] I. R. R. Peloso, A. Rodríguez, E. Carmona, K. Freitag, C. Jones, A. Stasch, A. J. Boutland, F. Lips, in *Inorg. Synth., Vol. 37* (Ed.: P. P. Power), John Wiley & Sons, Inc., **2018**, pp. 33–45.

[38] M. Westerhausen, M. H. Digeser, M. Krofta, N. Wiberg, H. Nöth, J. Knizek, W. Ponikwar, T. Seifert, *Eur. J. Inorg. Chem.* **1999**, 743–750.

[39] M. R. Crimmin, A. G. M. Barrett, M. S. Hill, P. B. Hitchcock, P. A. Procopiou, *Organometallics* **2007**, *26*, 2953–2956.

[40] K. X. Bhattacharyya, S. Dreyfuss, N. Saffon-Merceron, N. Mézailles, *Chem. Commun.* **2016**, *52*, 5179–5182.

[41] E. Espinosa, E. Molins, C. Lecomte, *Chem. Phys. Lett.* **1998**, *285*, 170–173.

[42] M. V. Vener, A. N. Egorova, A. V. Churakov, V. G. Tsirelson, *J. Comput. Chem.* **2012**, *33*, 2303–2309.

[43] M. J. Frisch, G. W. Trucks, H. B. Schlegel, G. E. Scuseria, M. A. Robb, J. R. Cheeseman, G. Scalmani, V. Barone, G. A. Petersson, H. Nakatsuji, X. Li, M. Caricato, A. V. Marenich, J. Bloino, B. G. Janesko, R. Gomperts, B. Mennucci, H. P. Hratchian, J. V. Ortiz, A. F. Izmaylov, J. L. Sonnenberg, Williams, F. Ding, F. Lipparini, F. Egidi, J. Goings, B. Peng, A. Petrone, T. Henderson, D. Ranasinghe, V. G. Zakrzewski, J. Gao, N. Rega, G. Zheng, W. Liang, M. Hada, M. Ehara, K. Toyota, R. Fukuda, J. Hasegawa, M. Ishida, T. Nakajima, Y. Honda, O. Kitao, H. Nakai, T. Vreven, K. Throssell, J. A. Montgomery Jr., J. E. Peralta, F. Ogliaro, M. J. Bearpark, J. J. Heyd, E. N. Brothers, K. N. Kudin, V. N. Staroverov, T. A. Keith, R. Kobayashi, J. Normand, K. Raghavachari, A. P. Rendell, J. C. Burant, S. S. Iyengar, J. Tomasi, M. Cossi, J. M. Millam, M. Klene, C. Adamo, R. Cammi, J. W. Ochterski, R. L. Martin, K. Morokuma, O. Farkas, J. B. Foresman, D. J. Fox, Wallingford, CT, **2016**.

[44] a) C. Lee, W. Yang, R. G. Parr, *Phys. Rev. B* **1988**, *37*, 785–789; b) A. D. Becke, *J. Chem. Phys.* **1993**, *98*, 5648–5652; c) P. J. Stephens, F. J. Devlin, C. F. Chabalowski, M. J. Frisch, *J. Phys. Chem.* **1994**, *98*, 11623–11627.

[45] a) R. F. W. Bader, *Atoms in molecules : a quantum theory*, Oxford University Press, New York, **1990**; b) *Chem. Rev.* **1991**, *91*, 893–928.

[46] a) P. R. Varadwaj, I. Cukrowski, H. M. Marques, *J. Phys. Chem. A* **2008**, *112*, 10657–10666; b) P. R. Varadwaj, A. Varadwaj, H. M. Marques, *J. Phys. Chem. A* **2011**, *115*, 5592–5601; c) A. K. Singh, M. Usman, G. Sciortino, E. Garribba, S. P. Rath, *Chem. Eur. J.* **2019**, *25*, 10098–10110.